

Organic & Biomolecular Chemistry

Accepted Manuscript



This article can be cited before page numbers have been issued, to do this please use: A. Ornelas, K. N. Williams, K. Hatch, A. Paez, A. C. Aguilar, C. C. Ellis, N. Tasnim, S. Ray, C. Dirk, T. Boland, B. Joddar, C. Li and K. Michael, *Org. Biomol. Chem.*, 2018, DOI: 10.1039/C7OB02198D.



This is an Accepted Manuscript, which has been through the Royal Society of Chemistry peer review process and has been accepted for publication.

Accepted Manuscripts are published online shortly after acceptance, before technical editing, formatting and proof reading. Using this free service, authors can make their results available to the community, in citable form, before we publish the edited article. We will replace this Accepted Manuscript with the edited and formatted Advance Article as soon as it is available.

You can find more information about Accepted Manuscripts in the [author guidelines](#).

Please note that technical editing may introduce minor changes to the text and/or graphics, which may alter content. The journal's standard [Terms & Conditions](#) and the ethical guidelines, outlined in our [author and reviewer resource centre](#), still apply. In no event shall the Royal Society of Chemistry be held responsible for any errors or omissions in this Accepted Manuscript or any consequences arising from the use of any information it contains.

Synthesis and Characterization of a Photocleavable Collagen-Like Peptide

Alfredo Ornelas,¹ Kaitlyn N. Williams,¹ Kevin A. Hatch,² Aurelio Paez,⁴ Angela C. Aguilar,² Cameron C. Ellis,³ Nishat Tasnim,⁴ Supriyo Ray,¹ Carl W. Dirk,¹ Thomas Boland,^{4,5} Binata Joddar,^{4,5} Chunqiang Li,^{2,5*} and Katja Michael^{1,5*}

¹Department of Chemistry and Biochemistry, The University of Texas at El Paso, 500 West University Avenue, El Paso, TX 79968, USA

²Department of Physics, The University of Texas at El Paso, 500 West University Avenue, El Paso, TX 79968, USA

³Department of Biological Sciences, The University of Texas at El Paso, 500 West University Avenue, El Paso, TX 79968, USA

⁴Department of Metallurgical, Materials and Biomedical Engineering, The University of Texas at El Paso, 500 West University Avenue, El Paso, TX 79968, USA

⁵Border Biomedical Research Center, The University of Texas at El Paso, 500 West University Avenue, El Paso, TX 79968, USA

*Corresponding Authors: kmichael@utep.edu; cli@utep.edu

Abstract

A 34 amino acid long collagen-like peptide rich in proline, hydroxyproline, and glycine, and with four photoreactive *N*-acyl-7-nitroindoline units incorporated into the peptide backbone was synthesized by on-resin fragment condensation. Its circular dichroism supports a stable triple helix structure. The built-in photochemical function enables the decomposition of the peptide into small peptide fragments by illumination with UV light of 350 nm in aqueous solution. Illumination of a thin film of the peptide, or a thin film of a photoreactive amino acid model compound containing a 5-bromo-7-nitroindoline moiety, with femtosecond laser light at 710 nm allows for the creation of well-resolved micropatterns. The cytocompatibility of the peptide was demonstrated using human mesenchymal stem cells and mouse embryonic fibroblasts. Our data show that the full-length peptide is cytocompatible as it can support cell growth and maintain cell viability. In contrast, the small peptide fragments created by photolysis are somewhat cytotoxic and therefore less cytocompatible. These data suggest that biomimetic collagen-like photoreactive peptides could potentially be used for growing cells in 2D micropatterns based on patterns generated by photolysis prior to cell growth.

Introduction

Collagen and collagen-derived materials have been used in tissue engineering applications, as these biomaterials form soft hydrogels that mimic the extracellular matrix providing structural support in which cells can grow, differentiate, and proliferate. The extracellular matrix is geometrically and topologically inhomogeneous,^{1,2} which are factors that modulate cell polarity and function.³ In the laboratory, collagen and gelatin can self-assemble in aqueous buffers resulting in hydrogels consisting of protein fibrils that form a porous mesh microstructure. The size of the fibrils, the density of the mesh, and the mechanical properties can be controlled by varying the pH, temperature, and ionic strength at which the hydrogel is prepared.⁴ For all of the reasons above collagens are attractive materials for biofabrication. In tissue engineering, biofabrication strategies typically include the development of scaffolds or composite constructs,

which exhibit tissue mimetic hierarchical features. Often the constructs include living cells or cell aggregates, bioactive molecules, or biomaterials that are printed and used for tissue fabrication.⁵ A list of the various techniques to print these cell-laden constructs has been published recently.⁶ While a plethora of technologies exist, the most common ones are extrusion pens,⁷ inkjet,⁸ electrospray,⁹ laser-induced forward transfer,¹⁰ and photopolymerization, for example the polymerization of poly(ethylene oxide) and poly(ethylene glycol)dimethacrylate to generate a hydrogel.¹¹ All have been adapted from the additive manufacturing field. For 2D cell patterning, a common technique is the patterning of scaffolds or cell adhesive domains via micro contact printing, in which a pattern is being etched into a silicon master, which is then used as a master for the printing process.¹² Another common technique for 2D cell patterning is inkjet printing. For example, a single-layer cellular micropattern was fabricated by printing an ink of primary embryonic hippocampal neurons in the pattern of a ring, with a 0.5 mm wide rim, 2.5 mm across, on a bio-paper substrate made from rat tail Type I collagen.¹³ While the 2D and 3D patterning processes described above rely on depositing cells on or into natural or unnatural polymers whose structures cannot be manipulated, we envisioned a new approach, i.e. a collagen-like peptide with unique properties, allowing for its site-specific decomposition at the microscale, creating short peptide fragments with potentially different properties than the bulk material. We hypothesized that the macroscopic material made from a collagen-like peptide with incorporated photoreactive moieties could be photolytically decomposed when illuminated at precise microscopic locations creating micropatterns.

Here we report a novel collagen-like peptide, with built-in photoreactive *N*-acyl-7-nitroindoline moieties and its characterization. We proposed that micropatterns could potentially be introduced into a biomimetic macroscopic bulk material by a photodegradation method, which could potentially guide tissue growth in specific 2D or even 3D patterns in the future. Recently, we showed the ability of such a photoreactive peptide (**1**) to undergo photolysis by a two-photon absorption process.¹⁴ Its two-photon photolysis products obtained by irradiation of a concentrated film had been verified by mass spectrometry,¹⁴ but the synthesis of peptide **1** had not been detailed out, and no further chemical or biological characterization had been conducted. Here we present the synthesis of this photoreactive 34 amino acid long collagen-like peptide (**1**) consisting of five hexapeptide repeats that are separated by the unnatural amino acid 5-carboxylic acid-7-nitroindoline (Figure 1), and the synthesis of the photoreactive amino acid building block. We also present studies on its secondary structure, its photolytic properties under UV light in an aqueous solution, its suitability for the generation of micropatterns using femtosecond laser photolysis, and its cytocompatibility with mesenchymal stem cells as well as mouse embryonic fibroblasts. In addition, we show that a 5-bromo-7-nitroindoline based amino acid, which can be easily synthesized from commercially available starting materials, also undergoes photolysis by a two-photon absorption process, and that it can serve as a model compound for more complex photoreactive 7-nitroindoline-based compounds with respect to patterning.

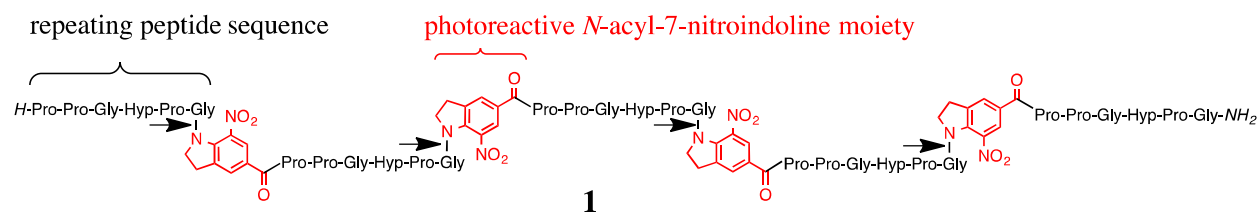
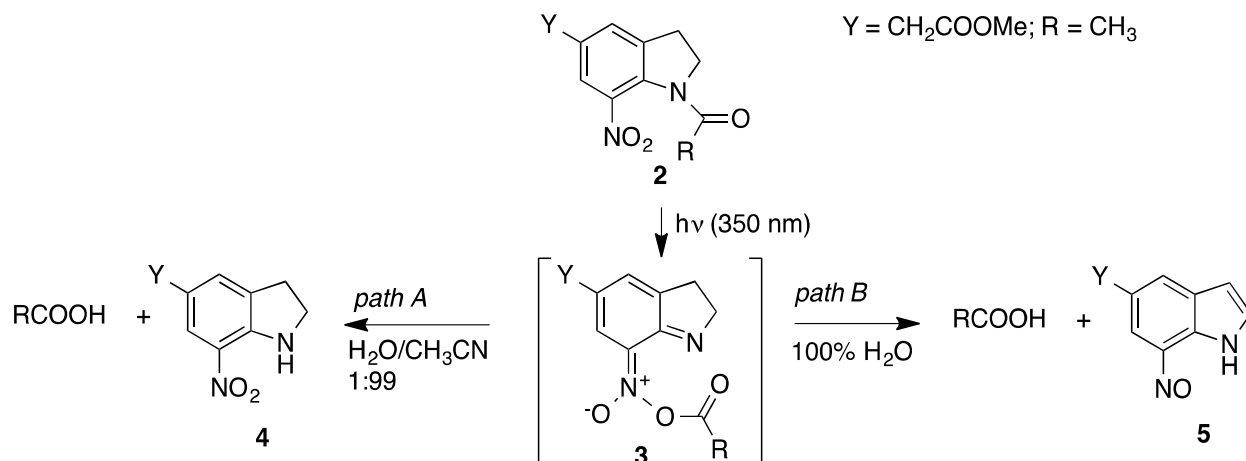


Figure 1. Photoreactive target peptide **1** with collagen-like repeating units and nitroindoline moieties (red) built into the peptide backbone. Photolytic cleavage occurs at the *N*-peptidyl-7-nitroindoline amide bonds indicated with arrows.

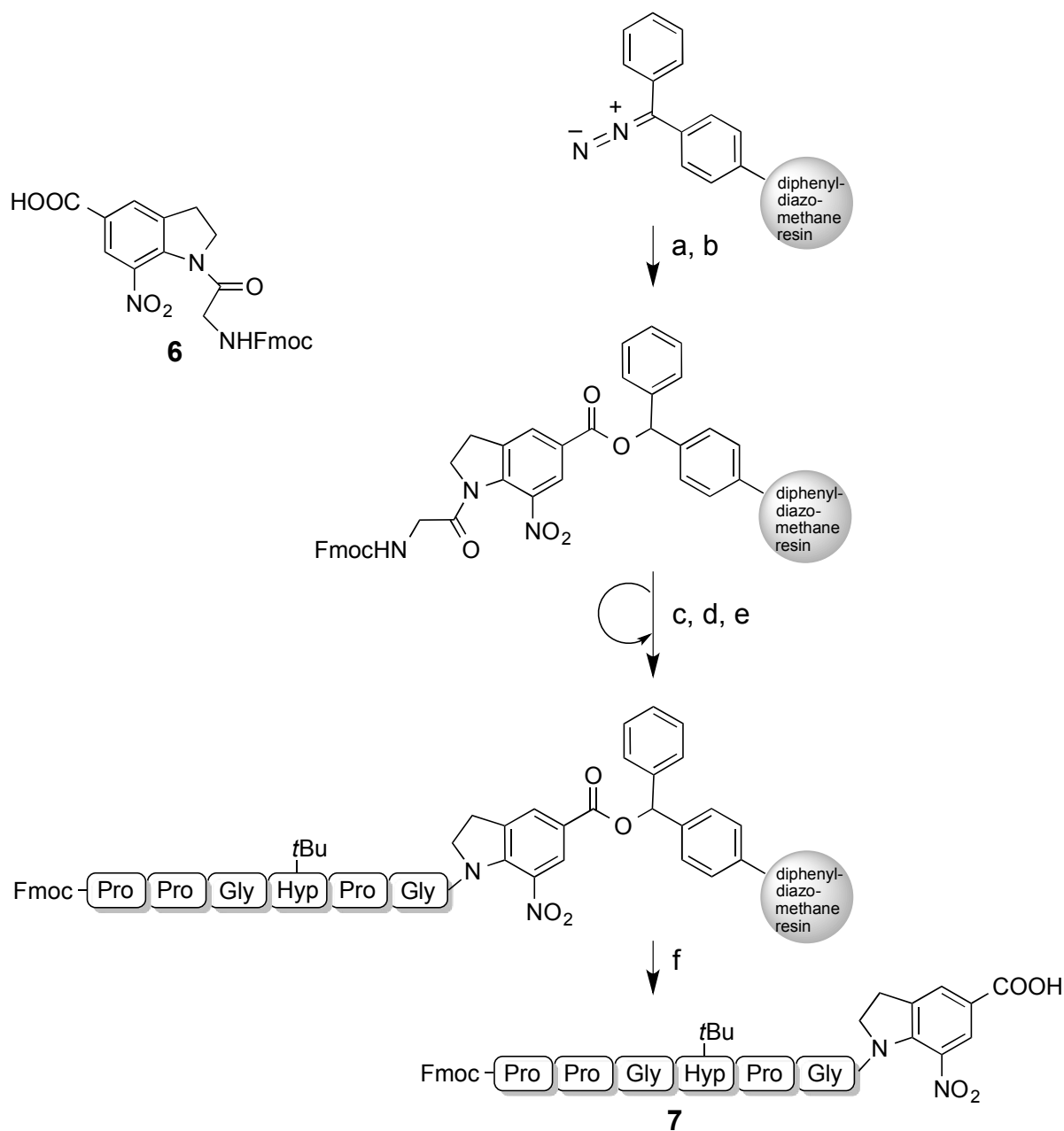
In designing a collagen-like peptide whose bulk material can potentially be modified by photolysis at precise locations, the following factors were considered: a) the amino acid components and length of the peptide; b) the photochemistry; and c) the synthetic strategy to access such a material. Collagens are major components in many extracellular matrices, and they play central roles in all phases of wound healing, including cell proliferation, remodeling, hemostasis, and inflammation.¹⁵ To mimic the properties of collagen and other collagen-mimicking peptides, which are typically about 30 amino acids long,¹⁶⁻¹⁹ we chose five hexapeptide repeats rich in glycine, proline, and hydroxyproline, with a glycine residue at every third position within the hexapeptide repeat. Since the ability to undergo photolytic cleavage into small peptide fragments was a required property, the design of the target peptide included four 7-nitroindoline moieties, which can be introduced via the photoreactive building block *N*-(Fmoc-Gly)-5-carboxylic acid-7-nitroindoline^{20, 21} in solid phase peptide synthesis (SPPS) using the Fmoc/*t*Bu strategy.²² In previous work we have shown that this building block is suitable for the installation of a photoreactive moiety at the C-terminus of peptides by SPPS, which can be photochemically converted into aliphatic or aromatic peptide thioesters and peptide hydrazides.^{20, 21} The photochemical properties of *N*-acyl-7-nitroindoline in an inert organic solvent in the presence of water, alcohols, or ammonia were first discovered more than 40 years ago and resulted in the acylation of these nucleophiles, producing carboxylic acids, esters, and amides.²³ Mechanistic studies of the underlying photochemistry suggest that upon light activation of the *N*-acyl-7-nitroindoline **2**, a nitronic anhydride intermediate **3** is formed,^{24, 25} possibly by a sigmatropic rearrangement.²⁶ In an inert organic solvent the nitronic anhydride **3** can either acylate a nucleophile, *e.g.* water, and produce a carboxylic acid and 7-nitroindoline **4** (Scheme 1, path A),^{24, 27} or form a carboxylic acid and nitrosoindole **5** in a photoredox reaction (path B, 100% water). The latter has been exploited for the photorelease of caged amino acids.²⁸ Which of the two paths predominates is solvent-dependent,²⁴ and is also influenced by the presence or absence of acid. For example, under acidic conditions, path B seems to be preferred, presumably due to protonation of the acyl oxygen of the nitronic anhydride intermediate **3**.²⁶ Other *N*-acyl-7-nitroindoline derivatives, with a bromo,^{23, 29-33} nitro,^{34, 35} or a carboxamido substituent^{20, 21, 36} at position 5 of the indoline ring, also undergo photoacylation (path A) with a number of different nucleophiles, including water, in inert organic solvents such as dichloromethane (DCM), acetonitrile, tetrahydrofuran, pyridine, *N,N*-dimethylformamide, *N,N,N',N'*-tetramethylurea, dimethylsulfoxide, and *N*-methylpyrrolidone. With respect to photoreactive peptide **1**, photolysis into small heptapeptide fragments with C-terminal glycine residues may occur by either pathway depending on the reaction conditions. We have recently shown that the photolysis of peptide **1** can also be accomplished by a two-photon absorption process.¹⁴ In that experiment, a highly concentrated thin film of peptide **1** in water was irradiated with femtosecond laser light at 710 nm. The mass-spectrometric analysis of the photolysis products showed that all expected peptide fragments formed, and that the photolysis had occurred via path A (Scheme 1) producing peptide fragments with *N*-terminal 7-nitroindoline moieties.¹⁴



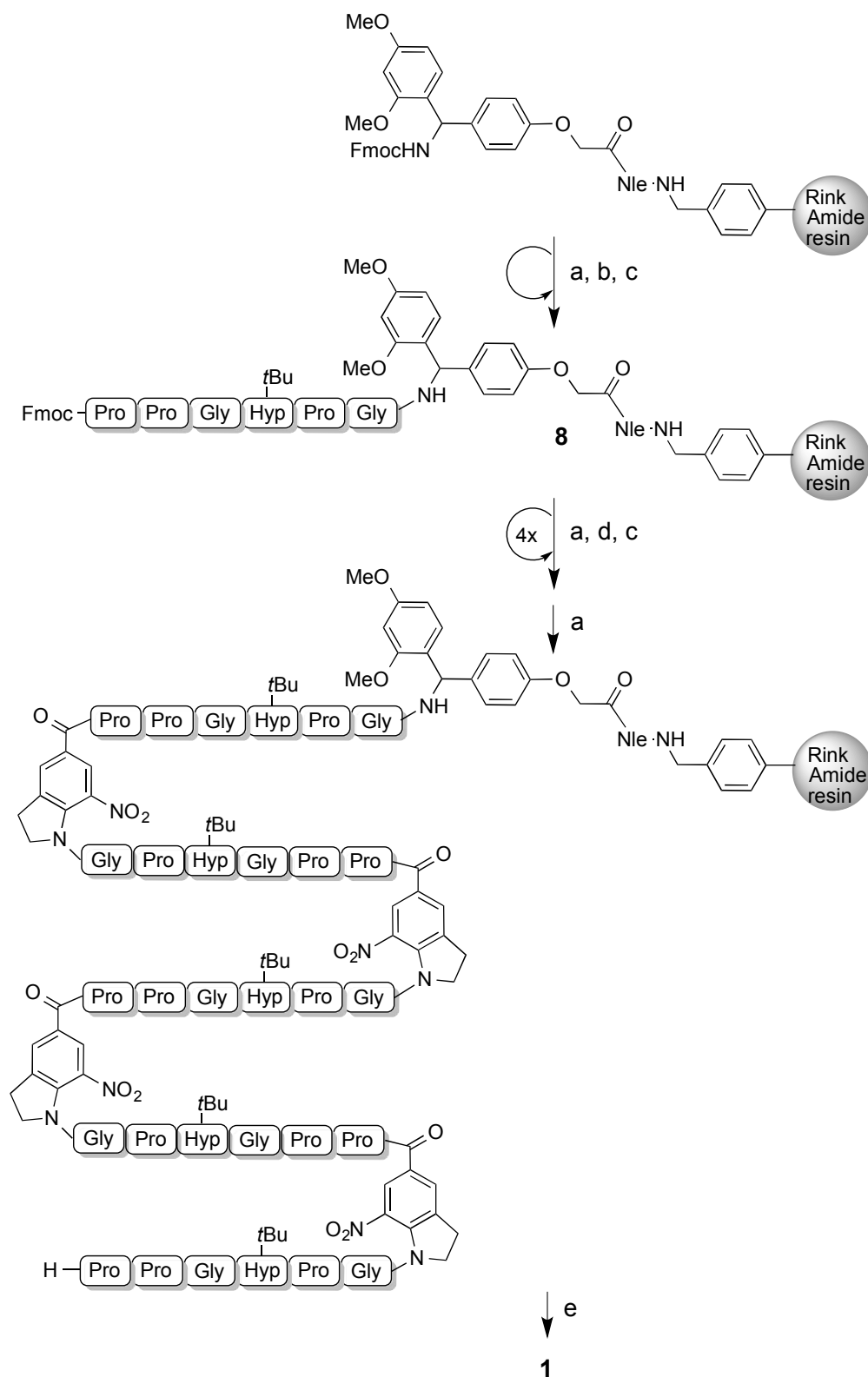
Scheme 1. Light activation of an *N*-acyl-7-nitroindoline and its solvent-dependent decomposition. A low water content favors path A, while a high water content favors path B.

Results and Discussion

Due to the five repeating hexapeptide sequences separated by four photoreactive moieties in peptide **1**, it lends itself to being synthesized by solid phase peptide synthesis (SPPS) using on-resin peptide fragment condensation. The photoreactive glycine building block **6** can be synthesized in seven steps from commercially available starting materials.^{20, 21} It was a key component in the synthesis of the protected photoreactive peptide segment **7** (Scheme 2), which was pre-prepared by SPPS on diphenyldiazomethane resin³⁷ for the fragment condensation. Since the attachment of the first amino acid to diphenyldiazomethane resin does not rely on activation with a coupling reagent, this resin is highly suitable for the recovery of unreacted amino acid excess, particularly when it is a precious building block such as the photoreactive glycine derivative **6**. The coupling of the remaining Fmoc-protected amino acids and the removal of Fmoc groups were accomplished under standard conditions using an uronium coupling reagent and *N*-hydroxybenzotriazole (HOBt) in the presence of *N,N*-diisopropylethylamine (DIPEA), and piperidine, respectively.²² The protected peptide acid **7** was cleaved from the resin with a dilute solution of trifluoroacetic acid in DCM. Scheme 3 shows the assembly of the photoreactive target peptide **1**. First, peptide **8** was synthesized by SPPS on Rink Amide resin followed by four on-resin fragment condensations using the pre-prepared photoreactive peptide **7**. Global deprotection and cleavage from the resin was accomplished with 95% trifluoroacetic acid (TFA), and purification of the peptide by reversed phase chromatography. Through a combination of semi-automatic Fmoc-SPPS and peptide fragment condensation, a 41% overall yield of peptide **1** was obtained. The peptide was characterized by mass spectrometry, UV-VIS spectrophotometry, fluorescence spectroscopy, and circular dichroism (CD). The peptide's ability to undergo photolytic cleavage with UV light in an aqueous solution was also investigated. Furthermore, in order to obtain preliminary cell toxicity information the peptide's ability to support the lateral growth of human mesenchymal stem cells, and its effect on the viability of mouse embryonic fibroblasts were studied.



Scheme 2. SPPS of the protected photoreactive peptide **7** on diphenyldiazomethane resin.
a) **6**, DCM; b) TFA/DCM; c) 20% piperidine/DMF; d) Fmoc-aa-OH, HBTU, HOBt, DIPEA, DMF (2×); e) Ac₂O, DIPEA, DMF; f) 3% TFA/DCM.



Scheme 3. Synthetic strategy for the preparation of photoreactive peptide **1** by on resin fragment condensation. a) 20% piperidine/DMF; b) Fmoc-aa-OH, HBTU, HOBT, DIPEA, DMF (2×); c) Ac₂O, DIPEA, DMF; d) **7**, TBTU, HOBT, NMM, DMF; e) TFA/H₂O/TIS 95:2.5:2.5.

Circular dichroism and thermal stability of peptide **1**

The far-UV CD spectra of peptide **1** show the typical signature of a triple helix (Figure 2a). The overall structure closely resembles the triple helices observed for collagen peptides that consist of naturally occurring amino acids.³⁸⁻⁴⁰ Increasing the temperature from 20 °C to 70 °C in 2 °C increments and then followed by 30 °C to 70 °C in 10 °C steps show practically no loss of structure (Figure 2a). Figures 2b and 2c show the mean molar ellipticity at $[\theta]_{200}$ and $[\theta]_{222}$, respectively, with the rise in temperature. There is minimal change in intensity both at 200 nm and 222 nm indicating that the secondary structure of the peptide is stable in the temperature range studied. Unlike other triple helical peptides of similar length,^{38, 41, 42} peptide **1** contains four units of the unnatural amino acid 5-carboxylic acid-7-nitroindoline, which could be responsible for its unusual stability. Unlike proteins that consist predominantly of α -helices or β -sheets, the CD spectra of collagen and gelatin have a strong minimum at approximately 200 nm which can be attributed to random coil structures and a positive peak at 222 nm, which is often not a pronounced maximum. Both are typical features of the CD spectra of collagen.⁴³ Importantly, the collagen-like structure formed by peptide **1** is very stable at 37 °C, which is highly significant as it enhances its utility for biological applications and its potential usefulness for cell adherence and growth.

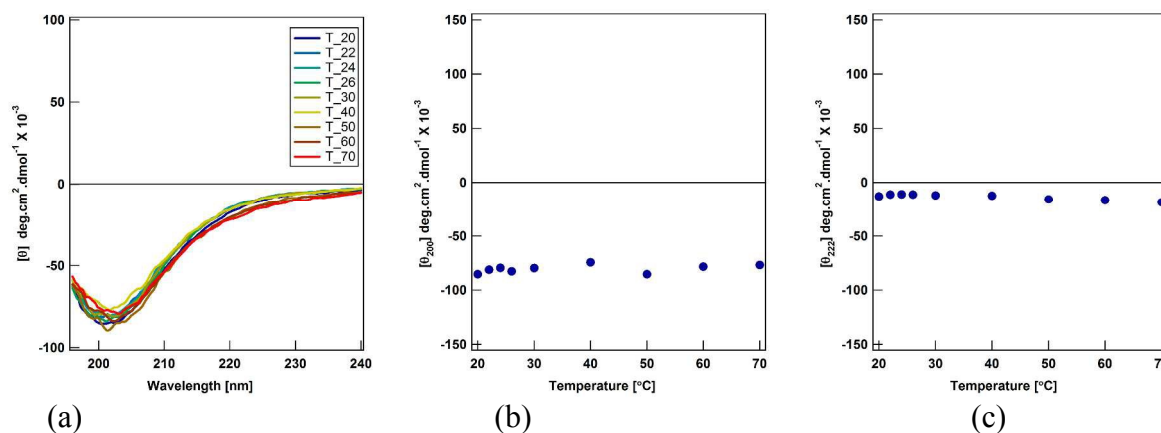


Figure 2. Secondary structure determination of the triple helical peptide using far-UV CD. a) The change in color from blue to red denotes the rise in temperature from 20 °C- 70 °C; b) Mean molar ellipticity at 200 nm at each temperature from 20 °C- 70 °C; c) Mean molar ellipticity at 222 nm at each temperature from 20 °C- 70 °C.

Photolysis of an aqueous solution of peptide **1** using UV light, and LC-MS analysis

In order to study whether or not peptide **1** is capable of undergoing photolysis at 350 nm light irradiation, an aqueous solution of **1** was illuminated for 5 min. The mass spectrometric analysis showed that starting material **1** was completely consumed. The three major peaks observed in the mass spectrum correspond to the N-terminal (**9**), middle (**10**), and C-terminal (**11**) peptide fragments. Peptide fragments **10** and **11** contain a 7-nitrosoindole moiety, which is in accordance with Corrie's solvent-dependence study (Scheme 1, path B).²⁴ However, a small peak that corresponds to a hexapeptide fragment with a nitroindoline (**12**) was also observed in this mass spectrum, suggesting that under the reaction conditions photolysis occurred by two pathways, albeit the expected reaction path (Scheme 1, path B) predominated. The peptide

mixture was also subjected to liquid chromatography-mass spectrometry (LC-MS) analysis. The data show that the photolysis of peptide **1** was complete; i.e., no large peptide fragments with intact photoreactive moieties were found. Also, peptides **9** – **12** are major photolysis products, with peptides **9** – **11** being most prominent. However, the total ion count (TIC) chromatogram appears to be complex and is consistent with the presence of peptide conformers, and several additional compounds. MS/MS analysis of three of these compounds suggests the presence of an unusual peptidyl-nitroindole and two peptidyl-nitrosoindolines (Electronic Supplementary Information).

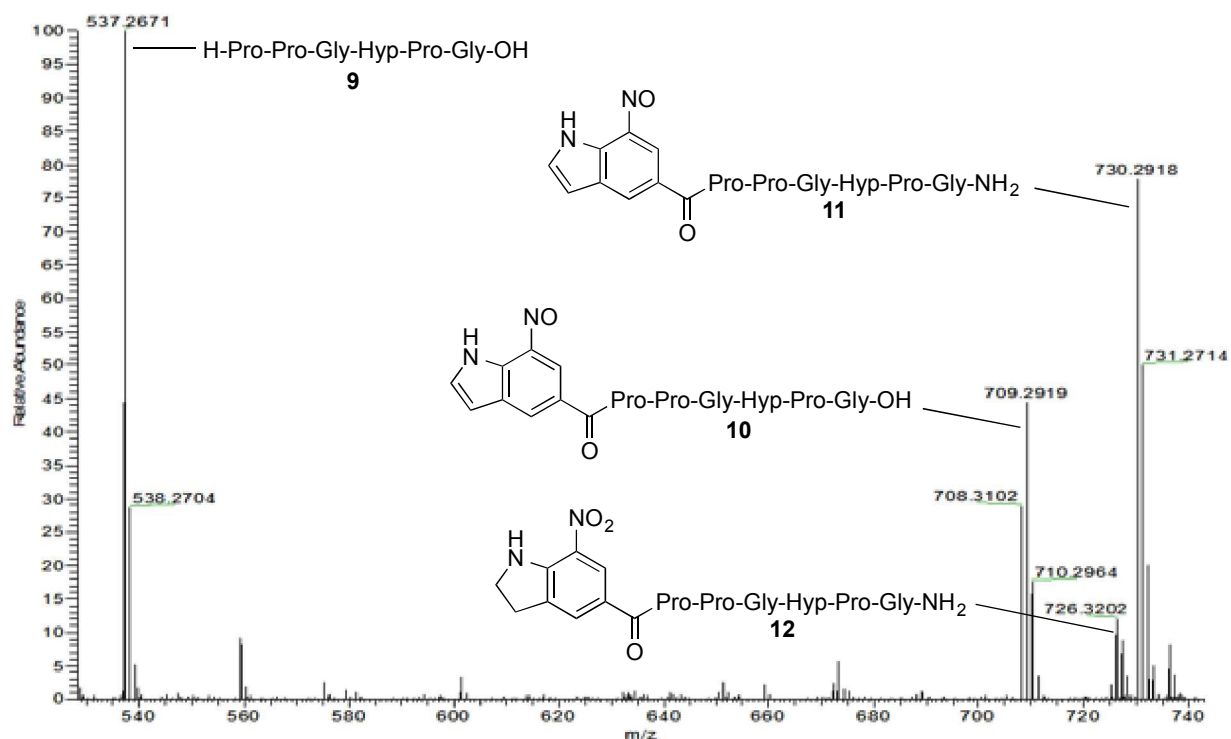


Figure 3. HR ESI MS after irradiation of peptide **1** with 350 nm light in water. Peptide **9**: m/z [M+H]⁺ calcd. 537.2672, obs. 537.2671; **10**: m/z [M+H]⁺ calcd. 709.2946, obs. 709.2919; **11**: m/z [M+Na]⁺ calcd. 730.2925, obs. 730.2918; **12**: m/z [M+H]⁺ calcd. 726.3211, obs. 726.3202.

Generation of a micropattern by two-photon absorption chemistry

In order to demonstrate the suitability of peptide **1** as a material for the generation of precise micropatterns using 710 nm femtosecond laser light, a nearly dry film of compound **1** was illuminated in a tree pattern with about 10 μm wide features. The illumination occurred through a mask of a tree in the optical path. This mask was made from a cover glass slip with a dark colored tape; only the tree, approximately 1 cm wide, was transparent. Only laser light that passed through the mask reached the film of the photoreactive peptide **1** in form of the tree pattern. Initially, the illuminated areas fluoresce (Figure 4 A-C), which triggers the photolysis resulting in non-fluorescent decomposition products such as peptides **9**, **12**, and other previously described photolysis products.¹⁴ Upon removal of the mask only the background consisting of intact peptide **1** fluoresces, and the tree appears dark (Figure 4, D). When viewed under a regular white light microscope, the light background color of compound **1**, and the orange color

of the photolysis products is clearly visible (Figure 4 E). The fact that the photolysis of peptide **1** only occurs at sites of illumination, and does not propagate through light-protected areas of the material, suggests that peptide **1** could potentially be suitable for photolithography and tissue engineering applications, such as matrix guided cell growth in distinct micropatterns.⁴⁴

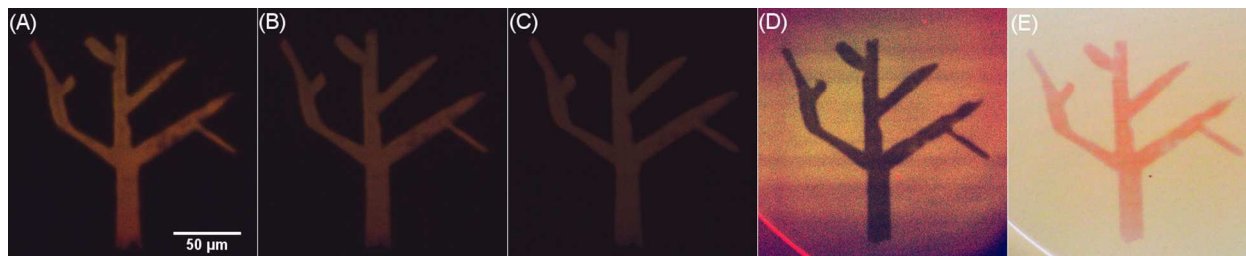


Figure 4. (A) Initial fluorescent tree pattern generated by two-photon excitation of the collagen-like peptide **1** with femtosecond laser at 710 nm light through a tree mask at time 0 min; (B) Fluorescent tree pattern after 10 min of irradiation, fluorescence decay is observed; (C) Tree pattern after 30 min of irradiation, fluorescence is barely visible due to progressive photolysis to non-fluorescent products; (D) After removal of mask and immediate recording of the fluorescence only the background fluoresces while the tree appears dark; (E) Tree under white light.

Photolysis of *N*-(Fmoc-glycyl)-5-bromo-7-nitroindoline (**13**) by a two-photon absorption mechanism

An important question was whether *N*-acyl-7-nitroindolines other than those with a carboxamido group at position 5 of the aromatic ring (as present in peptide **1**), or with a methoxy group at position 4,^{45, 46} also have the ability to undergo photolysis by a two-photon absorption mechanism. Using the photoreactive amino acid **13** (Figure 5) as a model compound, we investigated whether its photolysis could be achieved by a two-photon absorption mechanism using a femtosecond laser at 710 nm, and whether *N*-acyl-5-bromo-7-nitroindolines can undergo localized photolysis within a macroscopic film creating a specific micropattern. The one-photon absorption properties and release of carboxylic acids caged as *N*-acylated 7-nitroindolines have been reported in the literature.^{23,25,27,36} However, the photolysis of *N*-acyl-7-nitroindolines has never been investigated in the context of biopolymers, macroscopic materials, and thin films. After irradiation of a concentrated film of **13** with the femtosecond laser at varying laser powers ranging from 100 mW to 200 mW the formation of orange/brown spots indicates the formation of 5-bromo-7-nitroindoline (**14**) at the different irradiated sites. The observed color change was the first indication of a successful photolysis (Figure 5).

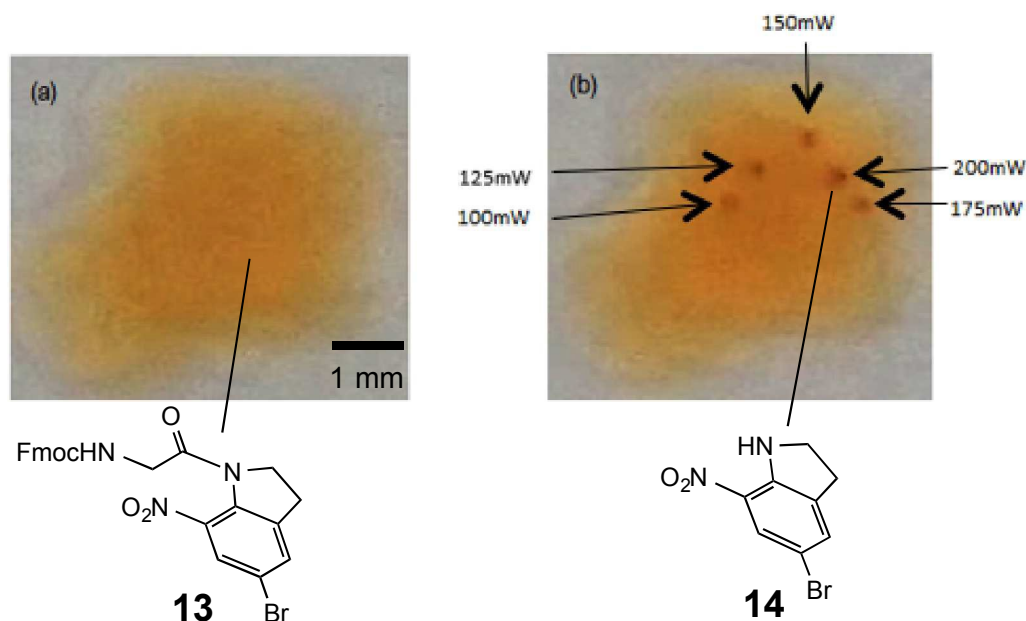


Figure 5. Images of a yellow film of *N*-[fluorenylmethoxycarbonyl-glycyl]-5-bromo-7-nitroindoline (**13**) before (a) and after (b) irradiation with a femtosecond laser at 710 nm at several locations with varying laser power (b). The photolysis produces orange/brown colored 5-bromo-7-nitroindoline (**14**) and colorless fluorenylmethoxycarbonyl-glycine.

Compound **13** exhibits a weak but measurable fluorescence, which is associated with its photochemical conversion into the non-fluorescent compound **14**. This unique property was exploited to investigate whether the photolysis occurs by a two-photon absorption mechanism using a fluorescence microscope. All the images produced were collected and analyzed using ImageJ³⁷ to measure the fluorescence intensity of individual channels. For each irradiated spot, a stack of images was created. An area was chosen within the image, and the average fluorescence intensity in each of the green and red channels was recorded. This measurement was performed in the same region of interest for every image in the stack, each taken one minute apart. A minimum fluorescence threshold was approximated for each image stack, and the fluorescence intensity normalized accordingly. A plot of these normalized intensities over time at varying laser powers from a single sample of **13** is shown in Figure 6. As it can be observed, the kinetics of the photoreaction are proportional to the intensity of the laser as the fluorescence decay is the fastest with the highest laser power (200 mW) and the slowest with the weakest laser power (100 mW).

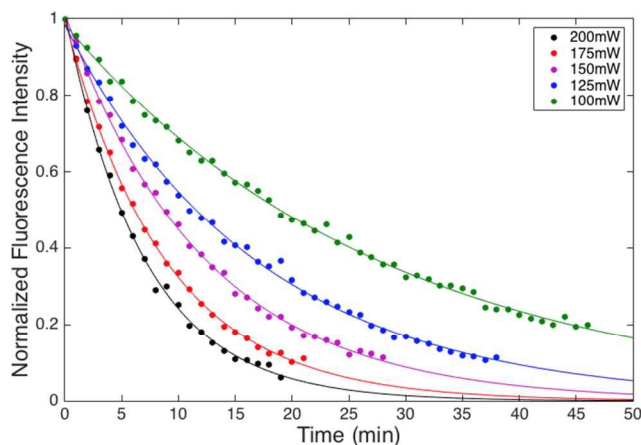


Figure 6. Fluorescence decay plots of compound **13** with exponential fitting at varying laser power.

These fluorescence decay plots may be modeled using an exponential decay regression line of the form $F(t) = Fe^{-\beta t}$, where β is the fluorescence decay rate. This was done using the curve fitting capabilities in Matlab. As mentioned before the fluorescence decay measured is directly proportional to the kinetics of the reaction. Therefore the fluorescence decay is equal to the rate of the reaction at every specific point and varying laser power. Since this photoreaction is occurring as a result of two-photon absorption, the rate of the reaction is directly proportional to the probability of two-photon absorption as shown in Eq. (1) where I is the excitation laser power.

$$\beta \propto I^2$$

Eq. 1 Probability of two-photon absorption, rate of reaction is proportional to the intensity of the laser squared.

Plotting a graph (Figure 7) where the x axis is the $\ln(I)$ and the y-axis corresponds to the $\ln(\beta)$ for each of the laser intensities employed and their corresponding decay rates produces a linear graph where the slope of the reaction has to be 2 to prove that a two-photon absorption process occurred. After plotting the graph, the slope observed was 1.996 (Figure 7), which clearly shows that compound **13** was photo-cleaved via a two-photon absorption process.

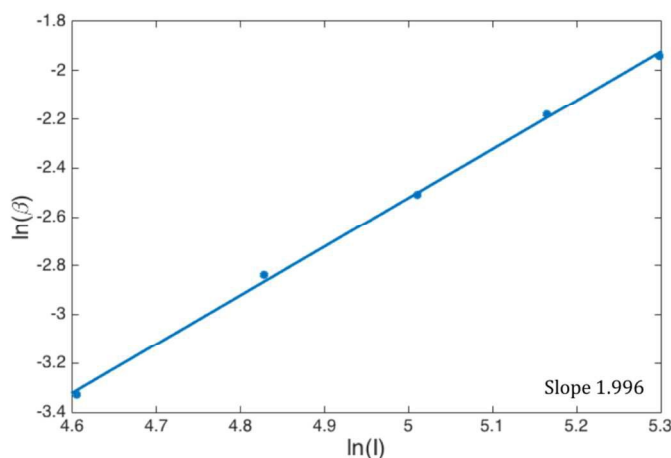


Figure 7. Double log plot of reaction rate vs. laser intensity for photoreactive compound **13**.

After irradiation the sample shown in Figure 5b was dissolved and analyzed by HR-ESI-TOF-MS, which showed the formation of 5-bromo-7-nitroindoline **14** (m/z $[M+H]^+$ calcd. 242.9769 and 244.9749, obs. 242.9784 and 244.9765, but not 5-bromo-7-nitrosoindole. The result is in accordance with Corrie's photolysis data, which show that the photolysis pathway depends on the water content of the sample (Scheme 1). He demonstrated that a similar *N*-acyl-7-nitroindoline in an inert organic solvent with only 1% water photolyzed to the nitroindoline.²⁴ Unlike our photolysis experiment of peptide **1** in water resulting predominantly in nitrosoindoles (Figure 3), compound **13** was irradiated as a highly concentrated, viscous film using non-anhydrous DMF as a solvent. This film contained small quantities of water, similar to Corrie's reaction conditions in Scheme 1, path A, allowing for the expected photo-hydrolysis to take place.

To test whether compound **13** could serve as an *N*-acyl-nitroindoline-containing model compound for the generation of micropatterns, an image of the logo of the University of Texas at El Paso ("UTEP") was projected on a thin film of compound **13** through a mask in the optical path of 710 nm femtosecond laser light. The experiment was conducted in a similar manner as described for the tree patterns shown in Figure 4. Initially, the illuminated areas fluoresce (Figure 8, left), which is associated with the photolysis to produce the non-fluorescent nitroindoline **14**. Upon removal of the mask only the background consisting of intact compound **13** fluoresces, and the logo appears dark (Figure 8, middle). When viewed under a regular white light microscope (Figure 8 right), the yellow background is due to the presence of compound **13**, and the orange-brown micropattern consists of compound **14**.



Figure 8. Left: Fluorescent logo of the University of Texas at El Paso generated by excitation of the photoreactive amino acid **13** with a femtosecond laser at 710 nm through a "UTEP" mask; middle: The letters of the logo underwent photolysis to the non-fluorescent nitroindoline **14**. After removal of the mask the background fluoresces; right: UTEP logo under white light.

Cytocompatibility

The cytocompatibility of peptide **1** was studied using human mesenchymal stem cells in a qualitative cell proliferation assay, and mouse embryonic fibroblasts in a Live/Dead assay. The latter assay also included the photolysis products of peptide **1**, and collagen as a control. Figure 9 illustrates that peptide **1** is not cytotoxic to cultured human mesenchymal stem cells as the cells showed viability and confluence within 24 hours of culture. Furthermore, peptide **1** promotes cell adhesion and migration. The blue line in the right image of Figure 9 denotes the edge of the immobilized peptide material from where undried/uncoated remnant liquid was aspirated prior to cell seeding. As the rim does not have any of peptide **1** immobilized, cells did not migrate, adhere or proliferate in that area, showing their preference to growing on the peptide-coated surface over the plastic of the well.

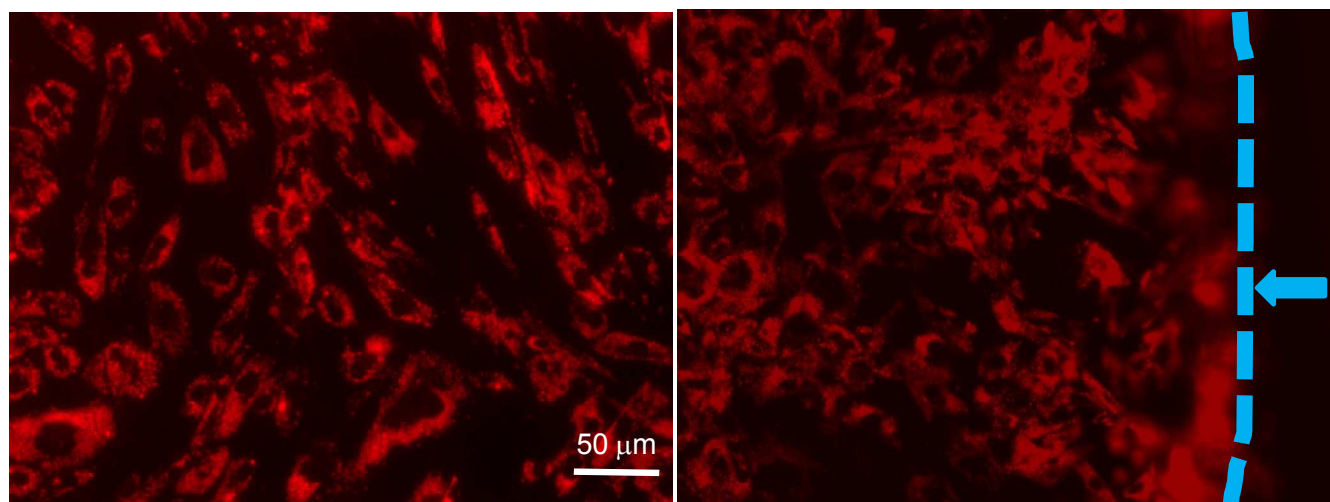


Figure 9. Human mesenchymal stem cells, pre-stained with PKH26, a cell membrane stain, and seeded atop collagen-like peptide **1** pre-immobilized onto tissue culture grade wells. Left: Images taken from center of the well. Right: cells grew only where the peptide sheet was present.

The cytocompatibility of peptide **1** and its photolysis products was also assessed using mouse embryonic fibroblasts by a Live/Dead cytotoxicity assay.⁴⁷ Figure 10A–C depicts confocal microscopy images of these cells cultured in wells coated with (A) peptide **1**; (B) peptide **1** irradiated with UV light; and (C) collagen as a control. The green fluorescence indicates live cells, and the red fluorescence indicates dead cells. The fibroblasts retained their viability and expressed their normal spindle shaped morphology⁴⁸ on the peptide coated (A) and collagen coated (C) surfaces. However, on the surface coated with the irradiated peptide (B), the fibroblasts do not show spindle shaped morphology, and most of the cells are dead.

To interpret the results of the Live/Dead cytotoxicity assay,⁴⁷ it is well known that live cells are distinguished by the presence of endogenous intracellular esterase activity, determined by the enzymatic conversion of the nonfluorescent cell-permeant calcein AM to the intensely fluorescent calcein (green). Although the polyanionic dye calcein is well retained within live cells producing an intense uniform green fluorescence, it is also important to note the healthy morphology of the cells. In Figure 10, fibroblasts with the healthy spindle-shaped morphology are observed only in (A) and (C), but not in (B) where the live-stained cells appear rounded and shrunk in their morphology. Moreover, in (B) we observe cells co-stained with both fluorescent dyes, green and red. The red fluorescence is conferred by the ethidium homodimer-1 (EthD-1), which enters cells with damaged membranes and undergoes a significant enhancement of fluorescence upon binding to nucleic acids, thereby producing a bright red fluorescence in dead cells. EthD-1 cannot cross the intact plasma membrane of live cells. Therefore the presence of both stains, green and red, and the absence of normal spindle shaped morphology in cells imaged in (B) imply that these cells are in the process of dying due to the presence of a cytotoxic surface caused by the photolysis products of peptide **1**. Although a similar number and morphologies of live cells are noted in (A) and (C), more dead cells are noted in the collagen coated controls (C) compared with the surface coated with peptide **1** (A). Since a solution of peptide **1** was deposited onto the wells in several layers followed by drying it may have created a bulge with,

which may have caused an overall smaller number of cells adhering onto this surface. However, the cells that did attach retained their viability and morphology implying that peptide **1** created a non-cytotoxic surface (A). In the future, we would need to improve the method for creating smooth and leveled peptide surfaces for tissue engineering applications. In conclusion, the photolysis products of peptide **1** show a certain cytotoxicity when compared to the intact peptide **1** and collagen, making peptide **1** a potential candidate for patterned 2D cell growth.

In principle, a number of different compounds could be responsible for the cytotoxic effect observed in Figure 10 (B). Previously, it was shown that the photolysis of a concentrated film of peptide **1** results in a mixture of peptidyl-7-nitroindolines.¹⁴ Therefore, the irradiation of a dry but not anhydrous film of peptide **1** with UV light is expected to produce predominantly peptides **9**, **12**, and [5-carboxylic acid-7-nitroindoline]-Pro-Pro-Gly-Hyp-Pro-Gly (**17**). With the limited cytotoxicity data at hand, the cytotoxic effect observed cannot be ascribed to a particular compound. In general, depending on the water content of the peptide sample at the time of irradiation, several peptidyl-7-nitroindolines and peptidyl-7-nitrosoindoles are possible photolysis products with potential effects on cell viability. The cytotoxicity of the individual compounds is not known.

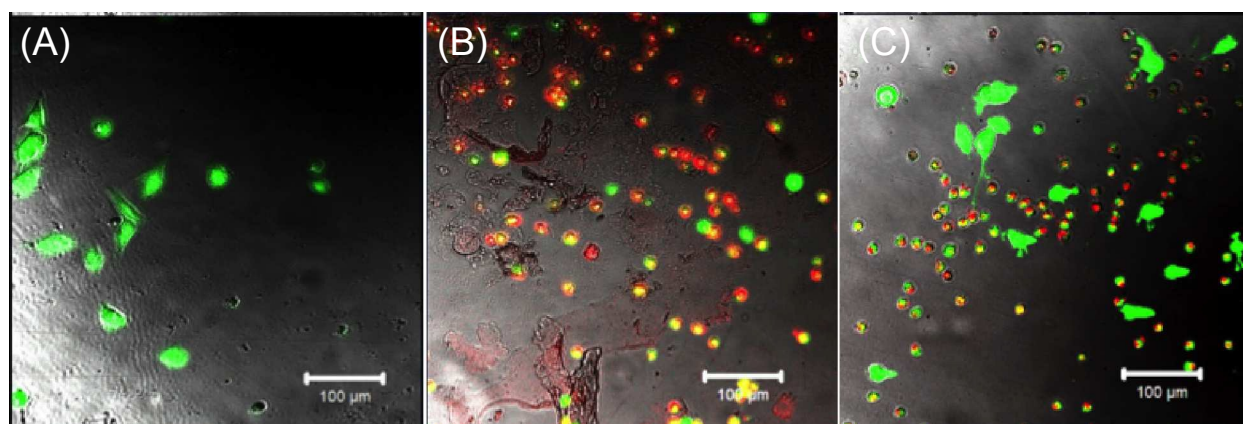


Figure 10. In the wells of a 96 well plate, mouse embryonic fibroblasts were seeded atop a surface coated with (A) non-irradiated peptide **1**; (B) irradiated peptide **1** resulting in its photodecomposition; and (C) collagen. Shown are representative merged images captured using bright field and fluorescence, where the green fluorescence depicts live cells and the red fluorescence indicates dead cells. The cells appear healthy and express their characteristic spindle shaped morphology atop the surface coated with peptide **1** (A). On the collagen coated surface (C), cells also express their ideal morphology, however, numerous dead cells are also noted. On the surface coated with peptide **1** that was irradiated with UV light prior to cell seeding (B), the cells are not found to express their ideal morphology and appear rounded. Also, very few live cells are observed.

Experimental

Reagents and Solvents

Fmoc amino acid derivatives were purchased from Anaspec Inc., BACHEM or Chem-Impex Intl. Inc. Diphenyldiazomethane resin and Rink Amide resins were obtained from BACHEM and Novabiochem, respectively. The coupling reagents HBTU and TBTU were purchased from

Anaspec Inc. and Novabiochem, respectively. HOBt, piperidine, and reserpine were obtained from Sigma Aldrich. Tetrakis(triphenylphosphine)palladium(0), N-methylaniline, N-methylmorpholine, TIS, and tetrachloro-p-benzoquinone were obtained from Acros. 5-Bromo-7-nitroindoline, thionyl chloride, and Ultramark were acquired from Alfa Aesar. Solvents, DIPEA, TFA, and bromophenol blue were obtained from Fisher Scientific. CDCl₃ and DMSO-d₆ were purchased from Acros and Cambridge Isotope Laboratories, respectively. Thin layer chromatography was performed on silica gel 60 F254 on aluminum (Merck). Column chromatography was performed on silica gel 60, 230-400 mesh from Natland International Corp.

Instrumentation

Peptides were synthesized semi-automatically using a Tribute peptide synthesizer from Protein Technologies, Inc. (USA). Reversed phase chromatography was performed on a Fast Protein Liquid Chromatography (FPLC) system in an AKTA Purifier from GE Healthcare Life Sciences. Superfrost microscope slides were obtained from Fisher Scientific (USA). UV-VIS absorption spectra were measured on a Shimadzu UV-3101PC UV-VIS-NIR scanning spectrophotometer using quartz cuvettes of 1 cm path length. Fluorescence spectra were measured on a Shimadzu RF-6000 spectrofluorophotometer using standard quartz cuvettes of 1 cm path length at rt. The fluorescence quantum yield was not determined. The excitation and emission bandwidths were 5 nm, and the Raman scattering of the solvent was subtracted. ¹H NMR and ¹³C NMR were recorded on a JEOL ECA-600 (600 MHz) or a Bruker Avance III HD (400 MHz). Tetramethylsilane was used as an internal standard. Mass spectrometry was performed on a high resolution JEOL Accu TOF mass spectrometer using an Electrospray Ionization (ESI) source or a High Resolution QExactive Plus-mass spectrometer from Thermo Fisher Scientific. The photolysis of peptide **1** in aqueous solution was performed in a Rayonet RPR200 photochemical reactor (USA) equipped with 16 UV lamps (350 nm). Far-UV Circular Dichroism (CD) studies were conducted using a Jasco-1500 spectropolarimeter connected to a Peltier temperature controller.

Synthesis

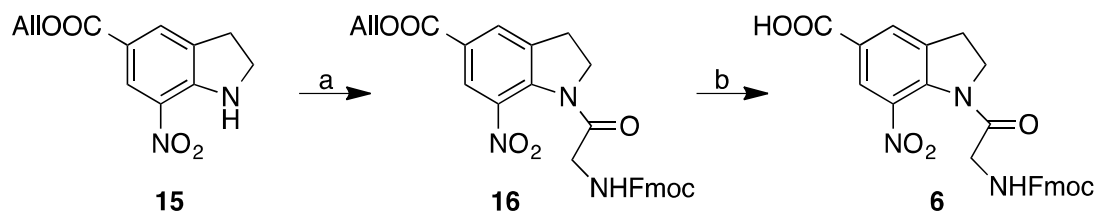
Peptide **1**

The photoreactive peptide **1** was synthesized from hexapeptide **8**, which was elongated by repeated coupling of pre-prepared peptide **7** by on resin fragment condensation. Hexapeptide **8** was synthesized on Rink Amide resin (loading capacity 0.62 mmol/g). The resin (0.059 mmol, 96 mg) was swollen in DCM (3 mL) for 30 min and washed 5 × with DMF. The resin's Fmoc group was removed with 20% piperidine in DMF (3 mL) under shaking for 15 min followed by washing with DMF (5 × 10 mL). Fmoc-Gly-OH (0.059 mmol, 18 mg, 1 equiv.), HBTU (0.059 mmol, 23 mg), HOBt (0.059 mmol, 8 mg) and DIPEA (0.118 mmol, 21 μL) were dissolved in DMF (0.12 M, 0.5 mL), immediately added to the resin and mixed for 45 min, then washed with DMF (5 × 5 mL) followed by capping with 10% Ac₂O, 5% DIPEA in DMF (3 mL, 15 min). The reason for using only ~ 1 equiv. of the first amino acid was to achieve an incomplete loading to reduce peptide aggregation during SPPS. Fmoc removal was accomplished as described before. The loading of the first amino acid onto the resin was 75% as determined by the quantification of dibenzofulvene by UV-VIS spectrophotometry (290 nm, ε₅₂₅₃, 1 cm. path length). The next five amino acids [Fmoc-Pro-OH, Fmoc-Hyp(*t*Bu)-OH, Fmoc-Gly-OH, Fmoc-Pro-OH, and Fmoc-Pro-OH] were coupled by dissolving 5 equiv. of the amino acid derivative (0.30 M), 5 equiv. HBTU, 5 equiv. HOBt and 10 equiv. of DIPEA in DMF, which was immediately added to the

resin, stirred for 15 min, double-coupled with half the quantities of the previous coupling step to furnish the resin-bound hexapaptide **8**. After capping and removal of the N-terminal Fmoc group as previously described, the peptide was further elongated by peptide fragment condensation (4 ×) with the photoreactive hexamer **7** (Scheme 3). For the fragment condensation, a solution of **7** (0.062 mmol, 62 mg, 2.5 equiv.), TBTU, 0.062 mmol, 20 mg), HOBt (0.062 mmol, 8 mg), and NMM 0.125 mmol, 14 μL) in NMP (0.10 M, 0.60 mL) was added to the resin and stirred for 9-11 hours. Coupling reactions were monitored with the bromophenol blue and chloranil tests,^{49, 50} and capping and removal of the N-terminal Fmoc group was performed as described before. The full length peptide **1** was cleaved off the resin with simultaneous side-chain deprotection using 95% TFA, 2.5% TIS, 2.5% water, 5 mL, 3 h, and the resin was washed twice with TFA. The crude peptide was concentrated under vacuum to a glassy film and precipitated with cold diethyl ether. The solution was centrifuged and the peptide pellet was washed several times with cold diethyl ether. The crude peptide **1** was dissolved in water and pre-purified by size exclusion chromatography on Superdex by isocratic elution with water. Final purification (48%) was achieved by reversed phase FPLC (Source) using a gradient of 10-35% (solvent A: 2% CH₃CN, and 0.1% TFA in H₂O; solvent B: 85% CH₃CN, and 0.1% TFA in H₂O. After lyophilization 75 mg of peptide **1** (49% with respect to the loading of the C-terminal amino acid) was obtained as a pale yellow solid. ESI TOF-MS *m/z* [M+2H]²⁺ calcd. 1685.7205 (most abundant species), obs. 1685.7175; [M+3H]³⁺ calcd. 1123.8061 (monoisotopic species), obs. 1123.8211. λ_{max} (H₂O, 29.7 μM) = 251 and 332 nm, ε₂₅₁ = 14297 M⁻¹ cm⁻¹, ε₃₃₂ = 2384 M⁻¹ cm⁻¹. λ_{em} (H₂O, 29.7 μM, excited at 332 nm) = 397 nm.

N-(Fmoc-glycyl)-5-carboxylic acid-7-nitroindoline (**6**)

The photoreactive glycine building block **6** suitable for SPPS was synthesized from nitroindoline derivative **15**²⁰ via glycine derivative **16** by Pd(0) catalyzed deallylation³⁵ (Scheme 4). In a round bottom flask, compound **16** (1.15 mmol, 0.61 g) and tetrakis(triphenylphosphine)palladium (0.12 mmol, 0.13 g) were dissolved in anhydrous tetrahydrofuran (THF, 10 mL) under argon. N-methylaniline (11.50 mmol, 1.25 mL) was added to the solution, which immediately turned dark red. The reaction was monitored by TLC until the starting material was consumed (1h). THF was removed under reduced pressure and the remainder was dissolved in ethyl acetate and washed extensively with a 1M HCl solution (10 × 50 mL), followed by water (5 × 50 mL), brine (2 × 50 mL) and dried over magnesium sulfate. Ethyl acetate was removed under reduced pressure to obtain an orange solid (0.56 g, quantitative) and no further purification was required. *R*_f = 0.18 (MeOH/DCM 5:95). ¹H NMR (400 MHz, 295 K, DMSO-d₆) δ 13.44 (s, 1 H, COOH); 8.10 (s, 1 H, H6); 8.08 (s, 1 H, H4); 7.90 (d, 2 H, ³*J* = 7.4 Hz, Fmoc-ArH); 7.78 (t, 1 H, NH); 7.75 (d, 2 H, ³*J* = 7.4 Hz, Fmoc-ArH); 7.42 (t, 2 H, Fmoc-ArH); 7.34 (t, 2 H, Fmoc-ArH); 4.33-4.30 (m, 4 H, Fmoc-CH₂, H2, H2'); 4.25 [t, 1 H, ³*J*_{Fmoc (CH/CH2)} = 7.0 Hz, Fmoc (benzylic)]; 4.10 (d, 2 H, ³*J*_{Hα/NH} = 6.0 Hz, Hα, Hα'); 3.29 (t, 2 H, ³*J*_{H2/H3} = 8.1 Hz, H3) ppm; ¹³C NMR (100 MHz, 295 K, DMSO-d₆) δ 168.2, 156.4, 143.8, 140.7, 139.3, 137.6, 136.5, 129.3, 127.6, 127.0, 125.2, 123.4, 120.0, 65.7, 48.8, 46.6, 43.6, 28.3 ppm. ESI-TOF-MS *m/z* [M-H]⁻ calcd. 486.1301; obs. 486.1327. λ_{max} (DCM, 41.1 μM) = 268, 301 and 324 nm, ε₂₆₈ = 18701 M⁻¹ cm⁻¹, ε₃₀₁ = 5092 M⁻¹ cm⁻¹, ε₃₂₄ = 1935 M⁻¹ cm⁻¹. λ_{em} (DCM, 82.1 μM, excited at 324 nm) = 392 nm.



Scheme 4. Synthesis of the photoreactive amino acid building block **6**: a) SOCl₂, toluene, 70°C; b) Pd(PPh₃)₄, *N*-methylaniline, THF.

Peptide 7

Diphenyldiazomethane resin (loading capacity 0.7 mmol/g, 0.99 mmol, 1.421 g) was swollen in 10 mL DCM in a peptide synthesis vessel for 20 min. The photoreactive building block **6** (0.995 mmol, 0.485 g) was dissolved in a DCM/DMF mixture (2:1) (0.20 M, 5 mL), added to the resin and in a peptide synthesizer shaken for 5 h. Upon completion of the coupling, the excess of compound **6** was recovered. The reason for using only ~ 1 equiv. of the first amino acid was to achieve an incomplete loading to reduce peptide aggregation during SPPS. After coupling of compound **6**, the resin was washed with DMF (5 × 10 mL), capped with 5 mL DCM/HOAc (1:1) for 1 h, and washed with DMF (5 × 10 mL). Fmoc removal was accomplished with 5 mL of 20% piperidine in DMF for 15 min followed by washing with DMF (5 × 10 mL). The loading of the first amino acid onto the resin was 47% as determined by the quantification of dibenzofulvene by UV-VIS spectrophotometry (290 nm, ε₅₂₅₃, 1 cm. path length). Fmoc-Pro-OH (4.97 mmol, 1.677 g), HBTU (4.97 mmol, 1.885 g) and HOBT (4.97 mmol, 0.671 g) were dissolved in DMF (1 M, 5 mL) and DIPEA (9.9 mmol, 1.73 mL) was added just before the solution was poured into the reaction vessel with the resin. The peptide reaction vessel was shaken for 15 min, followed by DMF washings (5 × 10 mL) and double coupling of the amino acid, with half the amounts of the previous coupling for 15 min. Capping was performed with 10% Ac₂O and 5% DIPEA in DMF (10 mL, 10 min). Using the same protocol, the peptide was elongated with the remaining amino acids in the order Fmoc-Hyp(*t*Bu)-OH, Fmoc-Gly-OH, Fmoc-Pro-OH, Fmoc-Pro-OH, except for that the N-terminal Fmoc group was not removed. Each coupling was monitored by the bromophenol blue test,⁵⁰ and chloranil test (preferred for N-terminal proline).⁴⁹ Peptide **7** was cleaved off the resin by repeated treatment with 3% TFA in DCM (10 mL) for 3 min until it was no longer visible in TLC (15 repetitions), then washed with fresh DCM (2 × 10 mL) and MeOH (2 × 10 mL). All peptide-containing fractions were combined, concentrated under reduced pressure to approximately 5 mL and precipitated with cold diethyl ether to obtain the crude photoreactive hexamer **7**. The suspension was centrifuged and the yellow pellet was washed several times with cold diethyl ether. The crude peptide was purified by silica column chromatography using a gradient of 5% MeOH to 10% MeOH in DCM to isolate peptide **7** (0.380 g) in 81% yield with respect to the loading of the first amino acid on the resin. *R*_f = 0.10 (5% MeOH in DCM). HR-ESI-TOF-MS *m/z* [M+H]⁺ calcd.: 1005.4358; obs. 1005.4334; [M+Na]⁺ calcd. 1027.4178; obs. 1027.4150. λ_{max} (DCM, 99.5 μM) = 267 and 327 nm, ε₂₆₇ = 10303 M⁻¹ cm⁻¹, ε₃₂₇ = 1103 M⁻¹ cm⁻¹. λ_{em} (DCM, 99.5 μM, excited at 327 nm) = 391 nm.

N-Fmoc-glycyl-5-bromo-7-nitroindoline (**13**)

This photoreactive amino acid was synthesized by acylation of commercially available 5-bromo-7-nitroindoline with Fmoc protected glycine chloride generated *in situ* using a procedure similar to a published method.²⁹ 5-Bromo-7-nitroindoline (2.00 mmol, 0.49 g, 1 equiv.) and Fmoc-Gly-

OH (3.00 mmol, 0.89 g) were suspended in anhydrous toluene (10 mL) under argon. The mixture was stirred at 70 °C for 15 minutes. Then thionyl chloride (8.00 mmol, 0.58 mL) was added dropwise which resulted in a clear solution after 30 min. The reaction was monitored by TLC until near completion (24 h). The solution was then diluted with ethyl acetate (250 mL) and washed with a saturated solution of NaHCO₃ (3 × 150 mL), water (3 × 150 mL) and brine (2 × 100 mL). The organic layer was dried over anhydrous MgSO₄, filtered and concentrated under reduced pressure. Compound **13** was purified by silica column chromatography (EtOAc:Hex 1:1); 0.940 g, 90% of an orange solid. *R_f* 0.18 (EtOAc:Hex 1:2); ¹H NMR (600 MHz, 295 K, CDCl₃) δ 7.76 (s, 1H, H6); 7.75 (d, 2H, ³*J* = 7.5 Hz, Fmoc, arom.); 7.59 (d, 2H, ³*J* = 7.5 Hz, Fmoc, arom.); 7.53 (s, 1H, H4); 7.38 (t, 2H, Fmoc, arom.); 7.29 (t, 2H, Fmoc, arom.); 5.82 (t, 1H, NH); 4.36 (d, 2H, ³*J*_{CH/CH₂} = 7.2 Hz, Fmoc-CH₂); 4.22-4.17 [m, 5H, H_α, H_α', H₂, H₂', Fmoc (benzylic)]; 3.22 (t, 2H, ³*J*_{H₂/H₃} = 8.0 Hz, H₃, H₃'). ¹³C NMR (150 MHz, 295 K, CDCl₃) δ 167.3, 156.7, 144.0, 141.6, 141.1, 138.7, 133.5, 132.2, 128.0, 127.4, 125.8, 125.5, 120.3, 117.4, 67.6, 49.1, 47.3, 44.5, 29.2. HR-ESI-TOF-MS *m/z* [M+NH₄]⁺ calcd. 539.0930 and 541.0913, obs. 539.0904 and 541.0937; [M+Na]⁺ calcd. 544.0484 and 546.0467, obs. 544.0489 and 546.0463. λ_{max} (CHCl₃, 76.6 μM) = 257 and 342 nm, ε₂₅₇ = 8968 M⁻¹ cm⁻¹, ε₃₄₂ = 651 M⁻¹ cm⁻¹. λ_{em} (CHCl₃, 23.7 μM, excited at 342 nm) = 383 nm, and 633 nm (weak), broadly emitted across the visible.

Allyl *N*-(Fmoc-glycyl)-5-carboxylate-7-nitroindoline (**16**)

5-Allyl carboxylate-7-nitroindoline (**15**)²⁰ was reacted with Fmoc-Gly-OH in the presence of SOCl₂ similar to a reported procedure.²⁹ Fmoc-Gly-OH (4.00 mmol, 1.189 g) and derivative **15** (2.00 mmol, 0.496 g, 1 equiv.) were suspended in anhydrous toluene (15 mL) under argon and warmed up to 70 °C. SOCl₂ (10.00 mmol, 0.73 mL) was added dropwise. After 60 min a clear solution was obtained. The reaction was monitored by TLC until near completion (40 h). The solution was diluted with ethyl acetate (200 mL) and washed with a saturated solution of NaHCO₃ (3 × 100 mL), water (3 × 100 mL) and brine (2 × 100 mL). The organic layer was dried over anhydrous MgSO₄, filtered and concentrated under reduced pressure. Product **16** was purified by silica column chromatography (EtOAc:Hex 2:1). An orange solid was obtained, 0.981 g, 93% .*R_f* = 0.13 (EtOAc:hexanes 1:1). ¹H NMR (600 MHz, 296 K, CDCl₃) δ 8.34 (s, 1 H, H6); 8.08 (s, 1 H, H4); 7.75 (d, 2 H, ³*J* = 7.5 Hz, Fmoc, arom.); 7.59 (d, 2 H, ³*J* = 7.5 Hz, Fmoc, arom.); 7.38 (t, 2 H, Fmoc, arom.); 7.30 (t, 2 H, Fmoc, arom.); 6.06-5.99 (m, 1 H, CH₂=CH-); 5.81 (t, 1 H, NH); 5.42 (dd, 1 H, ³*J*_{trans} = 17.2 Hz, ²*J* = 1.3 Hz, Allyl, olef. trans); 5.32 (dd, 1 H, ³*J*_{cis} = 10.4 Hz, Allyl, olef. cis); 4.84 (d, 2 H, ³*J*_{aliph./olef.} = 5.2 Hz, Allyl, aliph.); 4.37 (d, 2 H, ³*J*_{CH/CH₂} = 6.9 Hz, Fmoc-CH₂); 4.28 (t, 2 H, ³*J*_{H₂/H₃} = 8.1 Hz, H₂); 4.22-4.19 (m, 3 H, Fmoc (benzylic), H_α, H_α'); 3.29 (t, 2 H, H₃). ¹³C NMR (150 MHz, 296 K, CDCl₃) δ 167.3, 163.9, 156.3, 143.7, 141.2, 140.1, 137.5, 136.7, 131.6, 129.4, 127.7, 127.2, 127.1, 125.1, 125.0, 120.0, 119.1, 67.3, 66.3, 49.0, 47.0, 44.3, 28.7. HR-ESI-TOF-MS *m/z* [M+Na]⁺ calcd. 550.1590, obs. 550.1597; [M+K]⁺ calcd. 566.1330, obs. 566.1333. λ_{max} (DCM, 37.9 μM) = 258, 267 and 324 nm, ε₂₅₈ = 19461 M⁻¹ cm⁻¹, ε₂₆₇ = 17445 M⁻¹ cm⁻¹, ε₃₂₄ = 2192 M⁻¹ cm⁻¹. λ_{em} (DCM, 75.9 μM, excited at 324 nm) = 390 nm, tailing weakly through the visible.

Circular Dichroism (CD) of peptide **1** and thermal stability measurements

Far-UV CD experiments were conducted to study the secondary structure of peptide **1**. The measurements were carried out using a 20 μM solution of the lyophilized peptide **1** in 15 mM NaCl and 10 mM Na/K buffer (pH 6.8). The sample was placed into a quartz cuvette of 1 mm

path length (Jasco) and heated from 20°C - 70°C to characterize its thermal stability. At each temperature, the sample was equilibrated for 4 min prior measurement of the spectrum. CD scans were performed at a range of 196-240 nm with three accumulations of data at each temperature to improve the S/N ratio. Each spectrum underwent 11 point Savitzky-Golay smoothing to minimize high frequency noise. The experimentally estimated ellipticities (θ_{obs}) were converted to mean molar ellipticity $[\theta]$ using the formula: $[\theta] = (\theta_{\text{obs}})/ncl$ where l is the path length of the cuvette; c is the concentration of the peptide, and n is the number of stereogenic centers in the peptide.

Photolysis of an aqueous solution of peptide 1 at 350 nm and LC-MS/MS analysis

The photoreactive peptide **1** (2 mg) was dissolved in 2 mL of HPLC grade water (pH 7.3; 0.29 mM), placed into a plastic microcentrifuge tube and irradiated with ultraviolet light at 350 nm in a Rayonet photoreactor for 5 min at room temperature, followed by ESI-TOF mass spectrometric analysis of the crude reaction mixture. The photolysis products of peptide **1** were separated on an Aqua C18 column (5 μ m, 125Å, porous silica, Phenomenex) self-packed to a length of 25 cm, into a New Objective PicoTip Emitter (PF360-100-15-N-5. Tip 15 \pm 1 μ m). The Liquid Chromatography (LC) was performed on an UltiMate 3000 Dionex RSLCnano UHPLC (Thermo Fisher Scientific). The column was equilibrated in 95% Solvent A (100% H₂O, 0.1% formic acid), 5% Solvent B (90% acetonitrile, 10% H₂O, 0.1% formic acid), and maintained at a constant flow rate of 0.3 μ L/min throughout the run. A 5 μ L volume of the irradiated photolyzed peptide **1** sample at a concentration of 1 μ g/ μ L was loaded onto the column attached to a Nanospray Flex Ion Source (Thermo Fisher Scientific) for 5 min before beginning the gradient. Elucidation gradient of the photolyzed products consisted of an increase to 99% Solvent B over 31 min. A plateau of 99% Solvent B was maintained for 5 min, then brought down to 5% Solvent B for a 20-min re-equilibration with a total run time of 62 min. MS/MS data acquisition of the separated peptides was achieved using a Q Exactive Plus Hybrid Quadrupole-Orbitrap Mass Spectrometer (Thermo Fisher Scientific). The Q Exactive Plus was set to fragment the top 10 ions at full scan range of 300-1600 m/z (resolution of 70,000, AGC target 1e⁶) and dd-MS² (resolution at 17,500, AGC target at 1e⁵). The total ion chromatogram (TIC), mass spectra of individual eluting peptides, and MS/MS data can be viewed in the Electronic Supplementary Information.

Generation of a tree micropattern in a film of peptide 1

The photoreactive collagen-like peptide **1** (1 mg) was dissolved in 3 μ L of water and placed on a microscope slide. The solution was left to dry at room temperature in the dark for 12 h affording a thin film of **1**. The sample was covered with a coverslip and immediately used for the photolysis experiment. The tree mask was placed between the objective lens and the polygonal galvanometer to ensure the tree image was projected on the sample at the focal plane. The sample was irradiated under the two-photon microscope using 710 nm light with excitation laser output power of 200 mW. The delivered laser power at the sample location is 10% of this value, i.e., 20 mW. Upon excitation, the photoreactive peptide **1** emits a weak fluorescence, which decreases over time. Fluorescence images were recorded at 0, 10 and 30 min using a combination of red and green photomultiplier tubes. After removal of the mask another fluorescence image as well as an image using a white light microscope were recorded.

Laser set-up

The details of our in-house developed video-rate two-photon microscope was described in Reference.⁵¹ The light source is a mode-locked Ti:Sapphire laser (Maitai HP, 690-1040 nm, 100 fs, 80 MHz, Newport, Santa Clara, CA). We have used 710 nm light to achieve two-photon excitation of N-acyl-nitroindoline moieties. The home-built x-y scanner (polygon, galvanometer) has a 30 frames/s scanning rate. The laser power at the sample site is varied by rotating a half-wave plate in front of a polarizer. The fluorescence signal from the sample are detected in three spectral channels with photomultiplier tubes (PMTs, R3896, Hamamatsu, USA): red (570-616 nm, FF01-593/46, Semrock, USA), green (500-550 nm, FF03-525/50, Semrock, USA), and blue (417-477 nm, FF02-447/60, Semrock, USA). The outputs of these three PMTs are fed into red/green/blue channels of a frame grabber (Solios eA/XA, Matrox, Quebec, Canada). Two-dimensional images in the x-y plane are acquired through a home-built software program. Each frame has 500×500 pixels. Each final static image is an average of 30 frames. In the UTEP logo written experiment a photomask was placed at the intermediate image plane in the optical path, and the logo pattern was projected onto the objective lens focal plane to partially block the illumination light for pattern formation.

Two-photon excitation and photolysis of *N*-Fmoc-glycyl-5-bromo-7-nitroindoline (**13**)

The photoreactive amino acid **13** (2 mg) was dissolved in 2 μ L DMF to give a 1.92 M solution which was placed on a microscope slide. The solution was left to dry at room temperature in the dark for 30 min affording an approximately 70 μ m thick film of compound **13**. The sample was covered with a coverslip and immediately used for the photolysis experiment. Several spots within the sample were chosen for irradiation with the femtosecond laser at 710 nm, and each spot was irradiated with a specific excitation laser power (100 mW, 125 mW, 150 mW, 175 mW, or 200 mW). Upon excitation, the photoreactive amino acid **9** emits a weak fluorescence, which was collected using a combination of red and green photomultiplier tubes. The excitation triggers the photolysis of the glycine's amide bond, producing non-fluorescent Fmoc-glycine and 5-bromo-7-nitroindoline (**14**). As the photolysis progresses, the number of fluorescent molecules decreases, and consequentially a decrease in average fluorescence intensity at the irradiation site is measured. An image was taken every minute at each location and the fluorescence profile was tracked throughout the reaction. The location of each irradiated spot was recorded before a new spot was irradiated with a new laser excitation power.

Culture and passaging of human Mesenchymal Stem Cells (HMSC)

Human adipose derived mesenchymal stem cells were obtained from Lonza at passage 3 (Lonza, Allendale, NJ, USA) and cultured according to the manufacturer's recommendations. Certification was obtained and kept on file to ensure that the purchased HMSC were verified to be of the correct lineage and uncontaminated by other cell types or organisms. For the HMSC culture, a complete growth medium, specifically MSCGM HMSC growth BulletKit™ medium (Lonza), was used for maintaining the HMSC in an undifferentiated state. Prior to cell seeding, T-75 culture flasks were coated with 0.1% gelatin (Sigma Aldrich, St. Louis, MO, USA) and incubated (37°C, 1 h). After this, the cell suspension in medium was transferred to a gelatin coated T-75 flask and incubated for 1 h (37°C, 5% CO₂ and 95% RH). Prior to cell culture, the gelatin solution used for coating of the flasks was aspirated. After 70% confluency in culture was attained, cells were trypsinized and passaged for further experiments. The normal

morphology and phenotype of the cultured cells were confirmed by comparison with published images of HMSC Cells pre-stained with PKH26,⁵² a red fluorescent membrane staining dye (Sigma) following the manufacturer's protocols.

Human Mesenchymal Stem Cell (HMSC) growth on peptide 1

For testing the cytocompatibility of peptide **1**, ~1mg was dissolved in 100 μ L of distilled water and coated atop 24 wells of a tissue culture treated polystyrene dish and dried under a sterile laminar flow hood for 10-15 min prior to culture. HMSC were seeded atop this layer and cultured for 24 hours after which they were imaged using fluorescence microscopy (Zeiss Axiovision).

Mouse embryonic fibroblasts

Mouse embryonic fibroblasts, Sandos inbred mouse (SIM)-derived 6-thioguanine- and ouabain-resistant (STO) and growth inactivated by treatment with mitomycin-C (MITC-STO, Passage 6), were obtained from ATCC (<https://www.atcc.org/>; ATCC 56-X) and were employed to assess the cytocompatibility of peptide **1**, the photolysis products of peptide **1**, and collagen. These cells are feeder cells to support the growth of other cells such as stem cells^{53, 54} They have been treated with mitomycin-C and will not replicate, and thus serve as an ideal resource for cytotoxicity testing.⁴⁸

Live/Dead cytotoxicity assay of mouse embryonic fibroblasts on peptide 1, photolyzed peptide 1 and collagen

The peptide surfaces were prepared by dissolving 750 μ g of peptide **1** in 5 μ L of water/dimethylformamide (1:1) and pipetting 5 \times 1 μ L of this solution, 1 μ L at a time on top of each other, letting the solvent evaporate each time, in a well of a 96 well plate. For the irradiated peptide surface, a second well was prepared in the same manner, and the dried peptide film was then exposed to 365 nm of a 4W UV lamp for 3 h. A color change from pale yellow to orange was clearly visible indicating the photodecomposition of peptide **1** into its photolysis products. Collagen coated wells were prepared using a Rat Tail Collagen I solution (in 0.02 N acetic acid, concentration range 3 to 4mg/mL, Sigma-Aldrich). The collagen solution (1 mL) was diluted to a working concentration of 0.01% using sterile, tissue culture grade d.d. water. Next, the wells were coated with 100 μ L of this diluted solution and the protein was allowed to bind overnight at 2–8°C. Next, the excess fluid was removed from the coated surface and allowed to dry overnight. Prior to adding cells, the collagen-coated wells were rinsed with 1X PBS (3 times). About 15,000 cells were seeded per well (96 well plate, Nalgene-Nunc, Thermo-Fisher Scientific) along with 100 μ L of the complete growth medium on various substrates, including a) peptide **1**, b) the irradiated peptide **1**; and c) collagen. For cell culture, the cells were cultured in a humidified incubator (37 °C, 5% CO₂) using Dulbecco's Modified Eagle's Medium (DMEM) supplemented with 10% Fetal Bovine Serum (FBS) and 1% penicillin/streptomycin, all from Sigma-Aldrich. The 96-well plate was then placed back into the incubator to allow the cells to acclimate with the sample and kept undisturbed for 36 h. After this, the spent media was changed and the wells supplemented with fresh DMEM. At this point the wells were imaged to confirm cell adhesion onto the wells. Once cell adhesion was confirmed, the DMEM media was removed and the wells incubated with 100 μ L of the pre-warmed cytotoxicity reagent (Marker Gene Technologies Inc. Live:Dead Cytotoxicity Assay Kit Green/Red Staining).⁴⁷ The cells were then placed back into the incubator for 45 min. After incubation, the cells in wells were

washed using 1X PBS and imaged using light and confocal microscopy (ZEISS LSM 700 Confocal, Germany).

Conclusions

A photoreactive 30mer collagen-like peptide (**1**) with four photoreactive *N*-peptidyl-7-nitroindoline moieties was synthesized, and its photochemical and photophysical properties were studied. The temperature dependent circular dichroism spectra of this peptide provide the evidence of its folding into a triple helix similar to other collagen-mimicking peptides reported in the literature, and show an unusual structural stability, possibly due to the four units of the unnatural amino acid 5-carboxylic acid-7-nitroindoline in the peptide sequence. When an aqueous solution of peptide **1** is irradiated at 350 nm, photolysis occurs at all photoreactive amide bonds producing mainly the expected *N*-peptidyl-7-nitrosoindoles. When a thin film of peptide **1** is irradiated with a femtosecond laser at 710 nm through a patterned mask, micropatterns consisting of the photolysis products of peptide **1** are generated. The ability of *N*-glycyl-5-bromo-7-nitroindoline to also undergo photolysis by a two-photon absorption mechanism using a femtosecond laser at 710 nm and its suitability for generating well-resolved micropatterns was established. Since *N*-glycyl-5-bromo-7-nitroindoline is easily accessible from commercially available starting materials, in some aspects it can be used as a model compound for more complex *N*-acyl-7-nitroindolines such as peptide **1**. Qualitative cytocompatibility studies suggest that peptide **1** is not toxic to cells, as human mesenchymal stem cells were able to grow on a surface coated with that peptide, and mouse embryonic fibroblasts remained viable. In contrast, a surface coated with the photolysis products of peptide **1** exhibited a certain cytotoxicity to the fibroblasts. These data suggest that the photoreactive collagen-like peptide **1** has potential as a new biomimetic material that could be used for 2D patterned cell growth based on patterns generated by laser photolysis because of different cytotoxicity properties of peptide **1** when compared to its photolysis products.

Conflict of Interests

There are no conflicts of interest to declare.

Acknowledgements

This work was supported by the National Science Foundation, grant# DMR-1205302. Circular Dichroism data presented in this article was obtained with an instrument purchased with support from the National Institute of General Medical Sciences of the National Institutes of Health under linked award numbers RL5GM118969, TL4GM118971, and UL1GM118970. Optical experiments were supported by the National Institute of General Medical Sciences under grant# 1SC2GM103719, and by National Science Foundation under grant# DBI-1429708. This work was also supported by an interdisciplinary research grant of the University of Texas at El Paso (UTEP), Office of Research and Sponsored Projects. We thank Dr. Armando Varela for the cell images and acknowledge access to the LC-MS of the Biomolecule Analysis Core Facility at UTEP's Border Biomedical Research Center supported by the National Institute on Minority Health and Health Disparities, grant# 2G12MD007592.

Electronic Supplementary Information

Mass spectra of compounds **1**, **6**, **7**, **13**, and **16**; ^1H and ^{13}C NMR spectra of compounds **6**, **13**, and **16**, and FPLC of compounds **1** and **7**; LC-MS analysis of the photolysis products of compound **1** and MS/MS data of selected components.

References

1. C. Frantz, K. M. Sewart and V. M. Weaver, *J. Cell Sci.*, 2010, **123**, 4195-4200.
2. D. Han and P. I. Gouma, *Nanomedicine*, 2006, **2**, 37-41.
3. F. Berthiaume, P. V. Moghe, M. Toner and M. L. Yarmush, *FASEB J.*, 1996, **10**, 1471-1484.
4. M. Achilli and D. Mantovani, *Polymers*, 2010, **2**, 664-680.
5. J. Groll, T. Boland, T. Blunk, J. A. Burdick, D. W. Cho, P. D. Dalton, B. Derby, G. Forgacs, Q. Li, V. A. Mironov, L. Moroni, M. Nakamura, W. Shu, S. Takeuchi, G. Vozzi, T. B. Woodfield, T. Xu, J. J. Yoo and J. Malda, *Biofabrication*, 2016, **8**, 013001.
6. B. R. Ringeisen, R. K. Pirlo, P. K. Wu, T. Boland, W. Sun, Q. Hamid, Y. Huang and D. B. Chrisey, *MRS Bulletin*, 2013, **38**, 834.
7. L. Ouyang, R. Yao, Y. Zhao and W. Sun, *Biofabrication*, 2016, **8**, 035020.
8. T. Xu, J. Jin, C. Gregory, J. J. Hickman and T. Boland, *Biomaterials*, 2005, **26**, 93.
9. A. Abeyewickreme, A. Kwok, J. R. McEwan and S. N. Jayasinghe, *Integr Biol (Camb)*, 2009, **1**, 260-266.
10. N. R. Schiele, D. T. Corr, Y. Huang, N. A. Raof, Y. Xie and D. B. Chrisey, *Biofabrication*, 2010, **2**, 032001.
11. B. Dhariwala, E. Hunt and T. Boland, *Tissue Eng*, 2004, **10**, 1316-1322.
12. M. Fritz and M. Bastmeyer, *Methods Mol Biol*, 2013, **1018**, 247-259.
13. T. Xu, C. A. Gregory, P. Molnar, X. Cui, S. Jalota, S. B. Bhaduri and T. Boland, *Biomaterials*, 2006, **27**, 3580.
14. K. A. Hatch, A. Ornelas, K. N. Williams, T. Boland, K. Michael and C. Li, *Biomed. Opt. Express*, 2016, **7**, 4654-4659.
15. M. S. Agren, ed., *Functional Biomaterials*, Elsevier Ltd., Amsterdam, 2016.
16. S. M. Yu, Y. Li and D. Kim, *Soft Matter*, 2011, **7**, 7927-7938.
17. Y. Li and S. Yu, *Curr. Opin. Chem. Biol.*, 2013, **17**, 968-975.
18. V. Hernandez-Gordillo and J. Chmielewski, *Biomaterials*, 2014, **35**, 7363-7373.
19. J. Xiao, *Biophysical Characterization of Collagen Mimic Peptides*, Springer, Singapore, 1 edn., 2017.
20. T. J. Hogenauer, Q. Wang, A. K. Sanki, A. J. Gammon, C. H. Chu, C. M. Kaneshiro, Y. Kajihara and K. Michael, *Org. Biomol. Chem.*, 2007, **5**, 759-762.
21. A. Pardo, T. J. Hogenauer, Z. Cai, J. A. Vellucci, E. M. Castillo, C. W. Dirk, A. H. Franz and K. Michael, *ChemBioChem*, 2015, **16**, 1884-1889.
22. W. C. Chan and P. D. White, eds., *Fmoc solid phase peptide synthesis: a practical approach*, Oxford University Press, Oxford, 2000.
23. B. Amit, D. A. Ben-Efraim and A. Patchornik, *J. Am. Chem. Soc.*, 1976, **98**, 843-844.
24. J. Morrison, P. Wan, J. E. T. Corrie and G. Papageorgiou, *Photochem. Photobiol. Sci.*, 2002, **1**, 960-969.

25. A. D. Cohen, C. Helgen, C. G. Bochet and J. P. Toscano, *Org. Lett.*, 2005, **7**, 2845-2848.
26. J. E. Mendez, N. J. Westfall, K. Michael and C. W. Dirk, *Trends Photochem. Photobiol.*, 2012, **14**, 75-91.
27. G. Papageorgiou, D. Ogden, G. Kelly and J. E. T. Corrie, *Photochem. Photobiol. Sci.*, 2005, **4**, 887-896.
28. G. Papageorgiou, D. C. Ogden, A. Barth and E. E. T. Corrie, *J. Am. Chem. Soc.*, 1999, **121**, 6503-6504.
29. S. Pass, B. Amit and A. Patchornik, *J. Am. Chem. Soc.*, 1981, **103**, 7674-7675.
30. K. Vizvardi, C. Kreutz, A. S. Davis, V. P. Lee, B. J. Philmus, O. Simo and K. Michael, *Chem. Lett.*, 2003, **32**, 348-349.
31. O. Simo, V. P. Lee, A. S. Davis, C. Kreutz, P. H. Gross, P. R. Jones and K. Michael, *Carbohydr. Res.*, 2005, **340**, 557-566.
32. C. M. Kaneshiro and K. Michael, *Angew. Chem. Int. Ed.*, 2006, **45**, 1077-1081.
33. A. Hassner, D. Yagudayev, T. K. Pradhan, A. Nedelman and B. Amit, *Synlett*, 2007, 2405-2509.
34. C. Helgen and C. G. Bochet, *J. Org. Chem.*, 2003, **68**, 2483-2486.
35. J.-L. Débieux, A. Cosandey, C. Helgen and C. G. Bochet, *Eur. J. Org. Chem.*, 2007, 2073-2077.
36. K. C. Nicolaou, B. S. Safina and N. Winssinger, *Synlett*, 2001, **SI**, 900-903.
37. P. H. Chapman and D. Walker, *J. Chem. Soc. Chem. Commun.*, 1975, DOI: C39750000690, 690-691.
38. A. V. Persikov, Y. Xu and B. Brodsky, *Protein Sci.*, 2004, **13**, 893-902.
39. T. Koide, *Philos. Trans. R. Soc. Lond. B Biol. Sci.*, 2007, **362**, 1281-1291.
40. S. Frank, R. A. Kammerer, D. Mechling, T. Schulthess, R. Landwehr, J. Bann, Y. Guo, A. Lustig, H. P. Bachinger and J. Engel, *J. Mol. Biol.*, 2001, **308**, 1081-1089.
41. E. Leikina, M. V. Merts, N. Kuznetsova and S. Leikin, *Proc. Natl. Acad. Sci. U.S.A.*, 2002, **99**, 1314-1318.
42. F. W. Kotch and R. T. Raines, *Proc. Natl. Acad. Sci. USA*, 2006, **103**, 3028-3033.
43. R. Gopal, J. S. Park, C. H. Seo and Y. Park, *Int. J. Mol. Sci.*, 2012, **13**, 3229-3244.
44. B. Joddar, A. T. Guy, H. Kamiguchi and Y. Ito, *Biomaterials*, 2013, **34**, 9593-9601.
45. M. Matsuzaki, G. C. R. Ellis-Davies, T. Nemoto, Y. Miyashita, M. Iino and H. Kasai, *Nature Neurosci.*, 2001, **4**, 1086-1092.
46. G. Papageorgiou and J. E. T. Corrie, *Tetrahedron*, 2000, **56**, 8197-8205.
47. B. J. Kroesen, G. Mesander, J. G. t. Haar, T. H. The and L. d. Leij, *J. Immunol. Methods*, 1992, **156**, 47-54.
48. T. Murakami, I. Saitoh, E. Inada, M. Kurosawa, Y. Iwase, H. Noguchi, Y. Terao, Y. Yamasaki, H. Hayasaki and M. Sato, *Cell Med.*, 2013, **6**, 75-81.
49. T. Christensen, *Acta Chem. Scand. B* 1979, **33**, 763-766.
50. V. Krchňák, J. Vágner, P. Šafár and M. Lebl, *Collect. Czech. Chem. Commun.*, 1988, **53**, 2542-2548.
51. Y. Acosta, Q. Zhang, A. Rahaman, H. Ouellet, C. Xiao, J. Sun and C. Li, *Biomed. Opt. Express*, 2014, **5**, 3990-4001.
52. B. Joddar, S. A. Kumar and A. Kumar, *Cell Biochem. Biophys.*, 2017, DOI: 10.1007/s12013-017-0828-z. [Epub ahead of print].
53. Y. Zhou, H. Mao, B. Joddar, N. Umeki, Y. Sako, K.-I. Wada, C. Nishioka, E. Takahashi, Y. Wang and Y. Ito, *Sci. Rep.*, 2015, **5**, 11386.

54. B. Joddar, C. Nishioka, E. Takahashi and Y. Ito, *J. Mat. Chem. B*, 2015, **3**, 2301-2307.